Spring 5-1-2022

Characterizing Rat Lateral Amygdala Interneurons by Colocalization of Calcium-Binding Proteins via Serial Multiplex Immunohistochemistry

Ethan Gasteyer
ethan.gasteyer@uconn.edu

Characterizing Rat Lateral Amygdala Interneurons by Colocalization of Calcium-Binding Proteins via Serial Multiplex Immunohistochemistry

Ethan Michael Gasteyer

Undergraduate Honors Thesis

Department of Physiology & Neurobiology, University of Connecticut

Thesis Supervisor: Dr. Linnaea Ostroff

Honors Advisor: Susan Buraceski

April 29, 2022

Acknowledgements

I would like to thank the following people for helping to make this thesis project possible. From my initial training in the lab almost three years ago, all the way through the completion of this project, I am grateful to each of these individuals for contributing to my personal and academic growth.

Thesis Supervisor: Dr. Linnaea Ostroff

Honors Advisor: Susan Buraceski

Ostroff Lab Members (Current)

Janeth Perez-Garza

Gianna Raimondi

Jairo Orea

Emily Parrish

Murphy Kenny

Rebecca Tripp

Alison Chase

Mariel Agbim

Ostroff Lab Members (Former)

Zachary Deane

Peter Tiley

Advanced Microscopy Facility

Dr. Chris O'Connell

Table of Contents

Abstract

The lateral amygdala is a brain structure that plays an important role in regulating fear and anxiety. Some anxiety disorders are hypothesized to develop from failures in this local inhibitory circuit. Distinct populations of these inhibitory neurons express patterns of calcium-binding proteins and neuropeptides that suggest differences in functionality within the lateral amygdala. Furthermore, these patterns of expression are compared between male and female rats to identify sex differences in the lateral amygdala. Previous studies have reported sex differences in amygdala activation and connectivity, but very little is known about the sexual dimorphism of calcium-binding protein and neuropeptide expression.

These cell-type markers can be identified through immunohistochemistry, in which a target protein is tagged with a primary antibody, which is itself tagged and visualized with a fluorescent secondary antibody. While previous studies have explored this question through double-labeling, this study is unique in that it investigates the expression of these proteins through serial multiplex labeling. The advantage to serial multiplex labeling is that a single neuron can be labeled for ten or more cell-type markers, while previous studies have only been able to examine two or three at a time. Characterization of these subpopulations lends to a greater understanding of how the lateral amygdala functions within the fear and anxiety circuit and how the rat model can be applied to human neurobiology.

Introduction

The Amygdala

The amygdala is a brain region in the cerebral hemispheres of vertebrates, specifically the temporal lobe of primates and caudoventral forebrain of rodents, which regulates emotions (Pitkänen, 2000). Its dysfunction has been implicated in several human neurological and psychiatric disorders, such as anxiety, epilepsy, schizophrenia, depression, and Alzheimer's disease (Mears & Pollard, 2016). It can be subdivided into several nuclei (**Figure 1**), including the basolateral nuclear complex (BNC), which plays a significant role in processing sensory input in the context of fear conditioning and anxiety (Herry et al., 2010; LeDoux, 2000; Pape & Paré, 2010; Tovote et al., 2015). The BNC can be divided into lateral (LA), basolateral (BL), and basomedial (BM) nuclei, each with distinct roles within the fear and anxiety circuit. Each of these regions can be further subdivided along the ventro-dorsal and rostro-caudal axes (Paxinos & Watson, 1997).

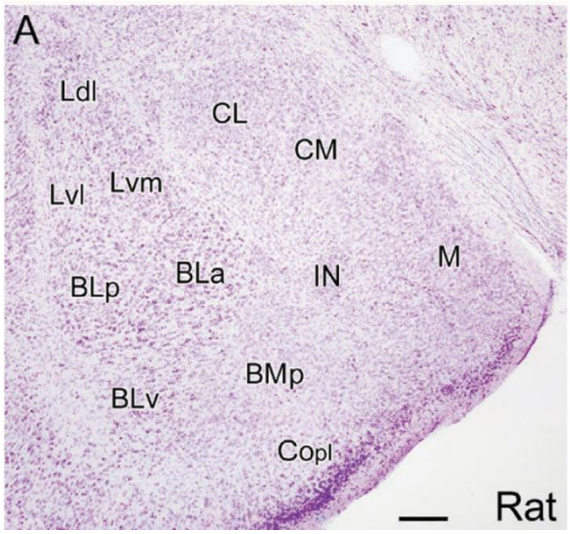

Figure 1. Nuclei of the rat amygdala. Ldl, Lvl and Lvm comprise lateral amygdala, BLp, BLa, BLv, and BMp comprise basal amygdala, CL and CM comprise central amygdala. Ldl = dorsolateral lateral, Lvl = ventrolateral lateral, Lvm = ventromedial lateral, BLp = posterior basolateral, Bla = anterior basolateral, BLv = ventral basolateral, BMp = posterior basomedial, Copl = posterolateral cortical, CL = lateral central, CM = medial central, IN = intercalated nucleus, M = medial (Image from McDonald, 2020).

Pyramidal Neurons

The projecting neurons of the LA are classified as pyramidal, similar to other brain areas such as the cortex. Their cell bodies measure about 10-35 microns across, with a single apical dendrite extending 400 to 700 microns from the cell body and 4 to 6 basal dendrites extending 5 to 20 microns. Level of branching varies greatly between neurons. The axons originate from the apical, basal, or lateral side of the cell body and project caudally (Hall, 1972; McDonald, 1982; 1984; Millhouse and DeOlmos, 1983). Pyramidal, or class I, neurons comprise about 85 percent of all LA neurons (McDonald, 1992) and are the main projection neurons from the LA to the prefrontal cortex and ventral striatum, utilizing excitatory neurotransmitters glutamate and aspartate (Fuller et al., 1987; McDonald, 1996; Smith and Paré, 1994). LA pyramidal neurons receive both inhibitory input at symmetric synapses via γ-aminobutyric acid (GABA) and excitatory input at asymmetric synapses via glutamate (Hall, 1972; Carlsen and Heimer, 1988; LeDoux et al., 1991; Stefanacci, et al., 1992; Smith and Paré, 1994; Brinley-Reed et al., 1995; Paré et al., 1995; Farb and LeDoux, 1999; Smith et al., 2000; Muller et al., 2006).

Non-Pyramidal Neurons

While pyramidal neurons have relatively consistent properties across the literature, non-pyramidal neurons vary greatly in morphology (McDonald and Augustine 1993; Paré and Smith, 1993; Lang and Paré, 1998; Smith et al., 2000). These class II and III LA cells comprise the population of interneurons, which provide most of the inhibitory input to pyramidal cells (Carlsen, 1988; McDonald et al., 2002). About one-quarter of non-pyramidal LA neurons are stellate cells. These have rounded cell bodies of about 10-15 microns in diameter, with 5 to 10

dendrites projecting in all directions and highly branched axons. Stellate cells typically are found singly and surrounded by pyramidal neurons. Another group of non-pyramidal neurons are known as cone cells, which have fusiform cell bodies about 20 to 25 microns wide and 30 to 35 microns long. These unusual cell bodies split into two or three branches before dividing into dendrites. Several other shapes and forms of interneurons have been identified in the LA that make this such a heterogenous group of cells (Millhouse and DeOlmos, 1983). There is some disagreement in the literature on where to draw the line between class II and III cells, but they are typically organized by size, with larger non-pyramidal cells comprising class II and smaller in class III. Neurogliaform cells, characterized by extensive branching of their axons, fall into class III (McDonald, 1992). The diversity of non-pyramidal interneurons is of particular interest to this study.

Many studies differentiate LA interneurons neurons based on patterns in molecular expression. This idea implies that neurons with different functions must have different intracellular components to accomplish these functions. Research has frequently targeted the expression of receptor proteins, neuropeptides, and calcium-binding proteins (McDonald and Pearson, 1989; McDonald and Mascagni, 2001a; Kemppainen and Pitkänen, 2000). Unfortunately, the specific functions of many of these molecules remain unknown, so the current literature mainly catalogs presence, trends, and immunoreactivity between the molecules.

Receptor Proteins

Receptor proteins are a physiologically important type of molecule that can be helpful in differentiating cell types. The presence or absence of a receptor can give insight into the cell's

function and also provide potential pharmacological targets. The main function of the amygdala is fear memory consolidation, so many studies investigate the receptors associated with this process. L-type voltage-gated calcium channels (VGCCs) are required for long-term potentiation (LTP), a key process in learning. The expression of a VGCC on an LA neuron could suggest it plays a role in LTP, which can be supported by behavioral tests. However, LTP also requires the expression of N-methyl-D-aspartate receptors (NMDARs) for fear acquisition. Expression of these two receptors can help identify potential subpopulations of neurons involved in these learning processes (Bauer et al., 2002). Other important receptors involved in LTP and fear memory formation include D2 dopamine receptors, CB1 cannabinoid receptors, group I metabotropic glutamate receptor subtype mGluR5, and serotonergic 5-HT receptors (Stutzmann and LeDoux, 1999; McDonald and Mascagni, 2001b; Rodrigues et al., 2002; Bissiere et al., 2003). Expression of receptor proteins in the LA is not investigated in this thesis. However, these listed are just a small sample of the receptor proteins expressed on LA cells and undoubtedly play a significant role in the functional differences of these neurons.

Neuropeptides

Neuropeptides are proteins found consistently in neurons having a range of functions including neurotransmission, modulation, and other signaling. Those found in highest concentration in the LA include vasoactive intestinal polypeptide (VIP), cholecystokinin octapeptide (CCK), somatostatin (SOM), and neuropeptide Y (NPY) (Roberts et al., 1982). Since GABA is a known inhibitory neurotransmitter, it is frequently used in studies to determine colocalization with these neuropeptides to identify trends and suggest possible associated functions. One study found that GABA-positive (GABA+) non-pyramidal cells were

immunoreactive for these neuropeptides in the following percentages: 14.3 percent SOM, 14.9 percent NPY, 17.4 percent VIP, and 7.9 percent CCK (McDonald and Pearson, 1989). This is just one example of the many studies investigating the colocalization of neuropeptides with GABA. Each GABAergic, neuropeptide-expressing cell can be considered as its own cell type and investigated for immunoreactivity with other neuropeptides and calcium-binding proteins.

Calcium-Binding Proteins

Calcium-binding proteins are found in high prevalence throughout the brain, but beyond binding to calcium, their exact function is not always clear. Since calcium is an important signaling molecule in the brain, there is a lot of speculation about the function of calcium-binding proteins. Like neuropeptides, they are also found in LA non-pyramidal neurons and exhibit immunoreactivity with GABA, notably parvalbumin (PV), calbindin-D28k (CalB), and calretinin (CalR). GABA+ LA cells were immunoreactive for these calcium-binding proteins in the following percentages: 41.2 percent CalB, 19 percent PV, and 20.5 percent CalR. A total of 57.8 percent of GABA+ neurons were immunoreactive for at least one calcium-binding protein (McDonald and Mascagni, 2001a).

As stated in the *Neuropeptides* section, each calcium-binding protein can be used to classify individual types of cells based on immunoreactivity with other molecules **(Figure 2**). One study defined three major subpopulations of GABAergic neurons in the LA: SOM+ neurons containing CalB and/or NPY, PV+ neurons containing CalB, and CalR+ neurons containing VIP (McDonald and Mascagni, 2002). It is important to note that these are general trends and do not describe every single GABAergic interneuron in the LA. CCK expression characterizes two

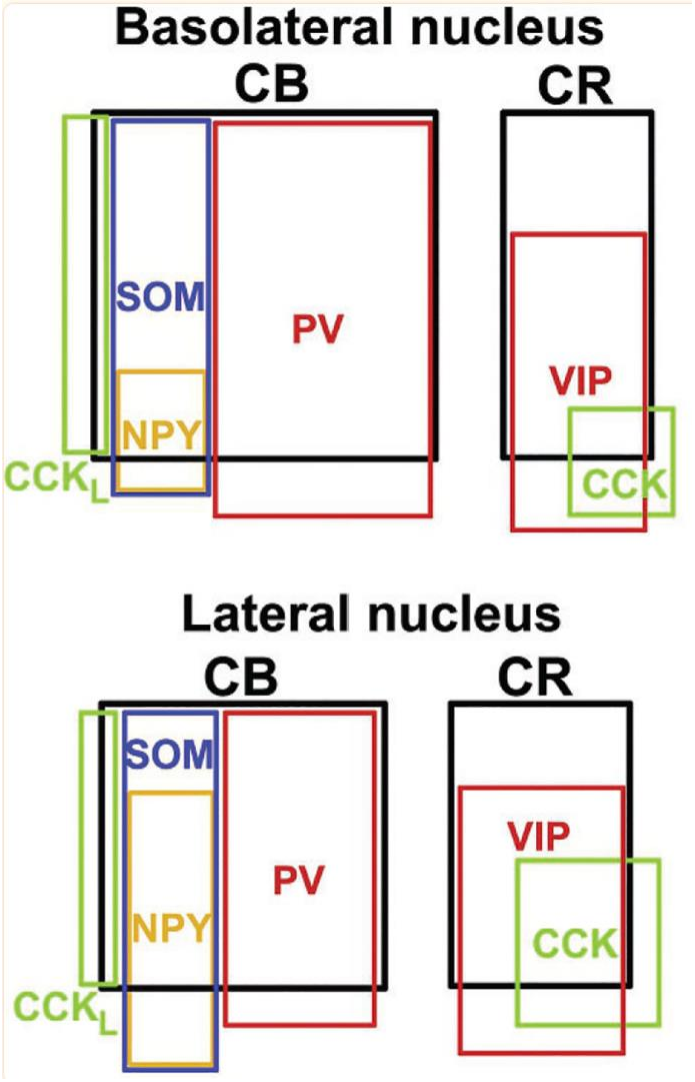

Figure 2. Overlap and relative ratios of GABAergic nonpyramidal neurons in rat basolateral and lateral amygdala nuclei. CB = calbindin, CR = calretinin, PV = parvalbumin, SOM = somatostatin, NPY = Neuropeptide Y, CCK = cholecystokinin, VIP = vasoactive intestinal peptide. (Image from McDonald, 2020).

major subpopulations of LA neurons: type L neurons, with large cell bodies and thick dendrites, and type S neurons, with small cell bodies and thin dendrites. Type L CCK+ neurons colocalized with CalB, but not PV, CalR, or VIP. On the other hand, type S CCK+ neurons colocalized with CalR and VIP, but not CalB or PV (Mascagni and McDonald, 2003).

This study examines the expression of CalB, CalR, and PV. Based on the work of McDonald, it was hypothesized that two major classes of LA interneuron would present. One type would be CalB+, some of which also express PV. The other type would be CalR+. These two populations should exhibit very low levels of overlap in expression (McDonald, 2020). While guided by McDonald's work, this thesis project is novel in its methods.

Sex Differences

Another important factor to consider in LA circuitry is the difference in expression between males and females. In humans, biological men and women exhibit different prevalence of psychiatric disorders, many of which involve the amygdala. For example, anxiety is diagnosed in 40.4% of adult women as opposed to 26.4% in adult men (Kessler et al., 2005; Kessler et al., 2012). Additionally, alcohol use disorder is twice as prevalent in men, and men tend to exhibit more severe symptoms (Substance Abuse and Mental Health Services Administration, 2019; Deshmukh et al., 2003; Erol & Karpyak, 2015). Some, but very few, projects have examined sex differences in calcium-binding protein expression. A few notable findings include higher expression of CalB+ interneurons in female guinea pigs and high colocalization of PV and estrogen receptor beta in the LA (Równiak et al., 2015; Blurton-Jones & Tuszynski, 2002). Blume et al. (2017) investigated LA differences between males and females, as well as differences within females at different stages of the estrus cycle: proestrous, characterized by high estradiol, and diestrous, characterized by low estradiol. The study examined many criteria, including morphology, electrophysiology, and PV expression. Significantly less PV+ cells were found in females than males, as well as less in proestrous than diestrous females. It is clear from these limited studies that the LA is sexually dimorphic in expression of calcium-binding proteins and further characterization is necessary (Blume et al., 2017). Through the methods described in this paper, male, proestrous female, and diestrous female rat LA sections can be processed at a high volume in a relatively short time to better identify these patterns and sex differences.

Dual-Labeling vs. Serial Multiplex IHC

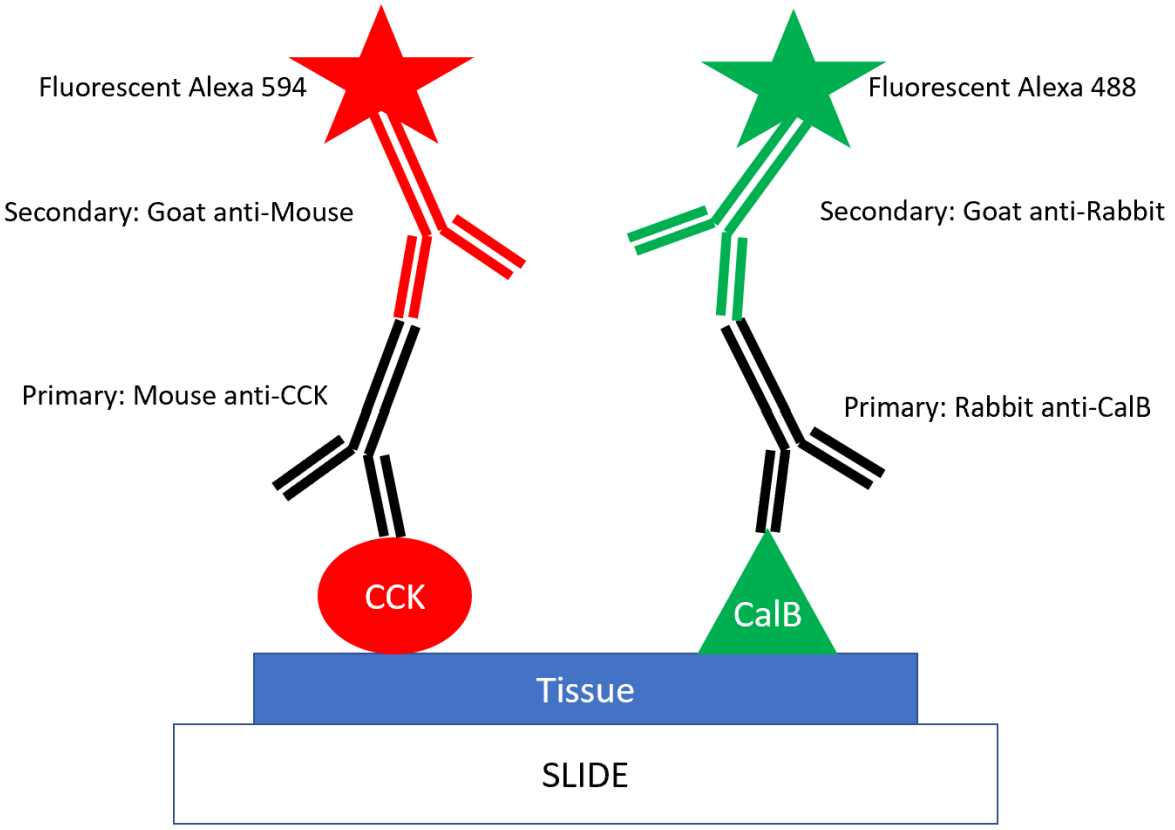

Figure 3. Example of dual-labeling immunohistochemistry procedure. In this example, the proteins of interest are cholecystokinin (CCK) and calbindin (CalB), whose antigens are represented by a red circle and green triangle, respectively. Primary antibodies bind directly to the antigens. Secondary antibodies then recognize and bind to the primary antibodies. The secondary antibodies are visualized by their conjugated Alexa Fluor markers.

McDonald identified these neuronal subpopulations through dual-labeling immunohistochemistry (IHC). In this method, the researcher applies two primary antibodies for two different protein targets to a single sample, usually 50 microns thick. For example, to identify CCK and CalB expression on a single sample, one could apply mouse anti-CCK and rabbit anti-CalB primary antibodies. The primary antibodies then must be visualized by fluorescent secondary antibodies, in this case Alexa-546 goat anti-mouse for CCK and Alexa-488 goat anti-rabbit for CalB **(Figure 3**). The Alexa-546 will mark CCK+ cells in a red channel, and the Alexa-488 will mark CalB+ cells in a green channel. Therefore, any cell expressing both

proteins will appear yellow when the two different color channels are overlapped (McDonald, 2021). While effective, this method has its limitations. For one, it is limited to identifying only two or three protein markers at a time. This is because in order for each to fluoresce a different color, its antibody must be from a different host species. In the previous example, CCK was a mouse antibody and CalB was a rabbit antibody. If each of these antibodies were only commercially available or proven to be effective in the same host species, it would be impossible to differentiate the expression of the two. This is a very likely dilemma, as only certain combinations of species to antibody are available, and the reliability of these antibodies to label exactly what they intend varies greatly.

To address this problem, this study employs serial multiplex IHC. For the exact procedure, refer to the *Materials and Methods* section, but the key difference is the thickness of the sample. McDonald typically used 50 micron-thick sections, while this study uses 100 nanometer ultrathin sections. This allows for up to 500 times more experiments to be done on the same region of tissue. The width of a typical neuronal cell body ranges from about 10 to 35 microns, so serial sections cut at 100 nanometers could theoretically allow for 100 or more sections through a single neuron. Because of this flexibility, each sample can be labeled with a different antibody without needing to avoid overlap of host species. For example, section 1 could use rabbit anti-CalB, section 2 could use rabbit anti-CalR, section 3 could use rabbit anti-PV, section 4 could use rabbit anti-VIP, section 5 could use rabbit anti-CCK, section 6 could use rabbit anti-NPY, and this could continue all the way through a single neuron with dozens of different antibodies. Alexa-488 goat anti-rabbit can then be used as the secondary antibody for all 4 sections, since they will be imaged and compared independently. This also eliminates the issue of different secondary antibodies exhibiting disparities in strength of fluorescent signal

incongruent to the levels of expression. One challenge with IHC is that false positive signal is very common and difficult to distinguish from real signal. By using the serial multiplex method, one can label consecutive sections with the same antibody to verify that the same neurons are labeled in both sections.

Materials and Methods

Animals and Tissue Preparation

An adult Sprague Dawley rat was perfused with 4% paraformaldehyde in 0.1M 1,4-piperazinediethanesulfonic acid (PIPES) buffer with 2mM $CaCl_2$ and 4mM $MgCl_2$. The tissue was microwave-embedded in 1:4 methyl-butyl methacrylate (MBA) resin. The MBA was prepared by adding 20 grams of methyl methacrylate to 80 grams of n-butyl methacrylate. This was mixed with dry nitrogen for 15 minutes. Next, 0.5 grams of benzoin methyl ether were mixed in for another 15 minutes in dry nitrogen. The tissue was dehydrated in increasing amounts of ethanol for 40 seconds at a time, at 37°C in a microwave. The dehydration solvent began as 50% ethanol in water for the first 40 seconds, then 70% ethanol for the next 40 seconds, 90% ethanol for 40 seconds, and finally two rounds of 100% ethanol for 40 seconds each. With the tissue fully dehydrated, resin infiltration began with a 1:1 solution of ethanol to MBA, which was microwaved for 15 minutes at 45°C. Two rounds of infiltration with 100% MBA followed, each for 15 minutes in the microwave at 45°C. Finally, polymerization took place in an Automatic Freeze Substitution (AFS) machine at 4°C under ultraviolet light for 48 hours.

Ultrathin Sectioning

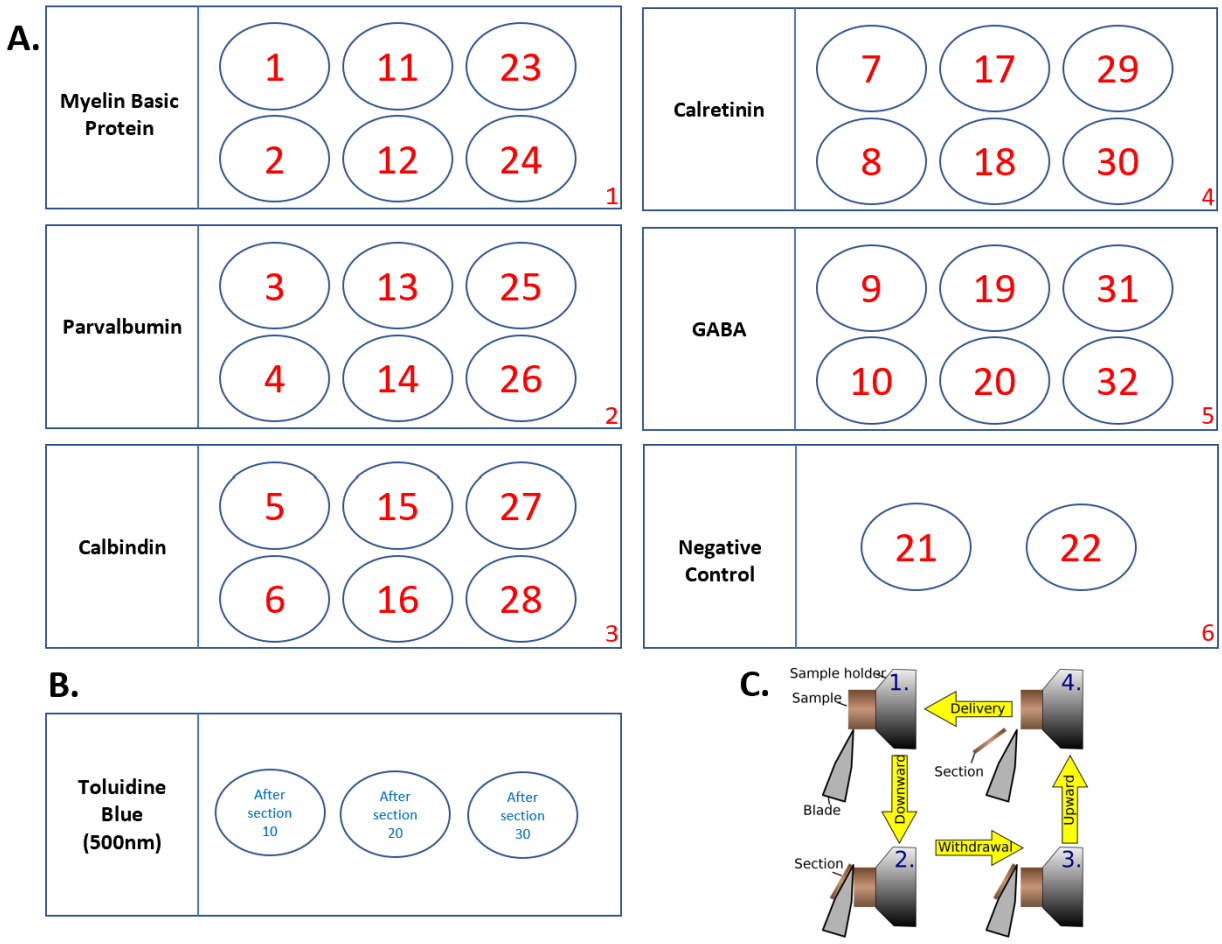

Figure 4. A, Arrangement of 100nm ultrathin serial sections 1-32 on subbed coverslips 1-6. All were processed for IHC as described in Methods. **B,** 500nm-thick sections taken immediately following sections 10, 20, and 30. Stained for Toluidine Blue on a subbed slide. **C,** Stepwise depiction of ultramicrotomy (Image from Ziel, 2013).

Sections were cut using a DiATOME Histo diamond knife on a Leica EM UC7 Ultramicrotome and placed on subbed 24mm x 60mm coverslips. Coverslips were prepared by dipping 5 times for 5 seconds each in gelatin-coating solution (0.5% gelatin, 0.05% chromium potassium sulfate dodecahydrate in 45°C deionized water). 100 nanometer ultrathin serial sections 1-32 were placed on slides 1-6 for IHC, according to **Figure 4**. After sections 10, 20, and 30, 500 nanometer-thick sections were placed on a subbed slide, to be stained for Toluidine Blue. Serial sections were warmed on a slide warmer at 60°C for 5 minutes. Toluidine Blue was

applied for one minute while warmed at 60°C. Slides were stored in a desiccator to keep sections dry.

Immunohistochemistry

The rinse solution (PBST) was 0.01M Phosphate-Buffered Saline, pH 7.4, with 0.1% Tween-20. The blocking solution was PBST with 1% Bovine Serum Albumin (BSA). This was used for the initial blocking step, as well as dilution of all primary and secondary antibodies. The primary antibodies for PV, CalB, and CalR target the calcium-binding proteins as previously described. The anti-GABA antibody identifies which cells are inhibitory (interneurons), as opposed to glutamatergic projecting neurons. Anti-Myelin Basic Protein (MBP) labels myelinated axons and is useful for delineating the boundaries of the LA. The negative control is not labeled with a primary antibody but does receive Alexa 488 goat anti-rabbit secondary antibody. This controls for any autofluorescence induced by the secondary in absence of primary.

Two slightly differing conditions were used for this experiment. For Slides 1-4 and 6 (stained for MBP, PV, CalB, CalR, and negative control), the following procedure was followed: Slides were immersed in 100% reagent grade acetone for 10 minutes to remove resin. The slides were then treated for antigen retrieval, by placing in an Instant Pot Pressure Cooker with 0.1M sodium citrate buffer, pH 6.0, for 10 minutes at “normal” pressure and “high” heat settings. The sections were then rinsed with PBST twice for 2 minutes each. BSA/PBST blocking solution was applied for 15 minutes. Immediately following blocking, primary antibodies (**Table 1**) were applied for 60 minutes. During the primary step, the negative control slide remained immersed in

BSA/PBST with no primary antibody. Sections were then rinsed with PBST twice for 2 minutes each. Secondary antibody (**Table 2**) was applied for 15 minutes. Sections were rinsed with PBST twice for 2 minutes each. The mounting medium, ProLong Gold Antifade Mountant with 4'6-diamidino-2-phenylindole (DAPI), was applied to each coverslip and flipped upside down to adhere to the glass slide. The procedure for slide 5 (GABA) had slight differences in the first steps. No acetone or pressuring cooking was done on this slide. Instead, sections were rinsed twice for 2 minutes each with PBST. Then, sections were immersed in 2% glutaraldehyde in PBST for 5 minutes. Sections were rinsed with 10mM glycine in PBST, three times for 2 minutes each. From this point on, the GABA slide joined slides 1-4 and 6 in rinsing, blocking, primary, secondary, and mounting steps. The only exception was that each subsequent rinse was done with the glycine/PBST solution, instead of just PBST like the other five slides. All slides were stored overnight in a dark refrigerator at 4°C.

Table 1. Primary antibodies and dilutions. All dilutions in BSA/PBST.

Antibody Target	Host Species	Dilution	Brand	Catalog #	Lot #
Myelin Basic Protein	Mouse	1:50	BioLegend	808401	B315597
Parvalbumin	Rabbit	1:1000	Abcam	Ab11427	GR3407557-2
Calbindin	Rabbit	1:50	SySy	214003	1-2
Calretinin	Rabbit	1:50	SySy	214102	1-4
GABA	Rabbit	1:50	Sigma	A2062	000011384712109121

Table 2. Secondary antibodies and dilutions. All dilutions in BSA/PBST.

2° Antibody	1° Antibodies Targeted	Dilution	Microscope Channel	Brand	Catalog #	Lot #
Alexa 488 Goat anti-Rabbit	PV, CalB, CalR, negative control	1:200	GFP	Invitrogen	A32731	VL315532
Alexa 488 Goat anti-Mouse	MBP	1:200	GFP	Invitrogen	A11001	2318440
Alexa 594 Goat anti-Rabbit	GABA	1:200	Texas Red	Invitrogen	A32740	WK333741

Imaging and Cell Counting

All slides were imaged on an Andor Widefield microscope with Nikon Eclipse Ti at 10x, 20x, 40x, and 100x. All slides were imaged in a DAPI fluorescent channel, which visualizes the nuclei of cells. Slides 1-4 and 6 were also imaged in a Green Fluorescent Protein (GFP) channel, which visualizes the labeling of Alexa 488 secondary antibodies. Slides 5 was imaged in a Texas Red channel, which visualizes the labeling of Alexa 594 antibodies.

Images were analyzed in ImageJ and aligned using an ImageJ plugin created by Ostroff Lab member, Alison Chase. Once aligned, the MBP slide was used to determine the boundaries of the BLA. Since MBP labels white matter, it shows a clear triangle-like shape that outlines the BLA. From there, a line was drawn from the internal capsule at the middle of the central amygdala, directly across BLA to the external capsule (**Figure 5**). This roughly divides the BLA into lateral and basal nuclei, however as described in *Introduction*, the exact boundary of the two nuclei is not well characterized in the literature. These boundaries could then be traced across all sections to make consistent cell counts. This was all done in close sections in order to maintain the same cells throughout the tissue. Since the same antibody was labeled on consecutive sections, many sections were redundant. As a result, the sections of each antibody with clearest labeling were used for cell counting. In this case, section 1 was used for MBP, section 4 for PV, section 6 for CalB, section 7 for CalR, and section 10 for GABA.

Next, total cell counts were made in the 20x DAPI channel images to determine the total number of cells contained within this slice of amygdala. Since DAPI labels all cells, this includes projecting neurons and glial cells in addition to interneurons. The GABA slide was used as the determinant of interneurons, since they are all GABAergic. CalB was the next cell type marker to be counted, because according to McDonald, it should constitute the largest population of

interneurons. PV was then counted, because it should exhibit high levels of colocalization with CalB. Finally, CalR+ cells were counted, and these should overlap with neither CalB nor PV. These counts were analyzed for colocalization with other calcium-binding proteins and expression patterns were compared with expected percentages based on previous studies.

Results

According to the DAPI labeling, there were 230 total cells in BA and 298 in LA. The Texas Red images showed that out of the 230 BA cells, 38 (16.52%) were GABA+ interneurons, and of the 298 LA cells, 34 (11.41%) were GABA+ interneurons. The GFP images showed that in the BA, there were 11 CalB+ cells out of the 38 interneurons (28.95%). In the LA, there were 6 CalB+ cells out of 34 interneurons (17.65%). The BA had 7 PV+ cells, which comprised 18.42% of interneurons and 63.64% of CalB+ cells. The LA had 3 PV+ cells, which were 8.82% of interneurons. Only 2 of the 3 PV+ LA cells also expressed CalB, accounting for 33.33% of LA CalB cells. All PV+ cells were also immunoreactive for CalB in BA. CalR was expressed in 4 BA cells, which was 10.53% of BA interneurons, and 4 LA cells, which was 11.76% of LA interneuronns. None of the CalR+ cells expressed CalB or PV. See **Table 3**, **Figure 5**, and **Figure 6**.

Table 3. Breakdown of calcium-binding protein expression in GABAergic interneurons.

Nucleus	Calcium-Binding Protein (CBP)	# of CBP+ cells	# of GABA+ cells	% of GABA+ cells expressing CBP
Basal	Calbindin	11	38	28.95%
	Parvalbumin	7		18.42%
	Calretinin	4		10.53%
Lateral	Calbindin	6	34	17.65%
	Parvalbumin	3		8.82%
	Calretinin	4		11.76%

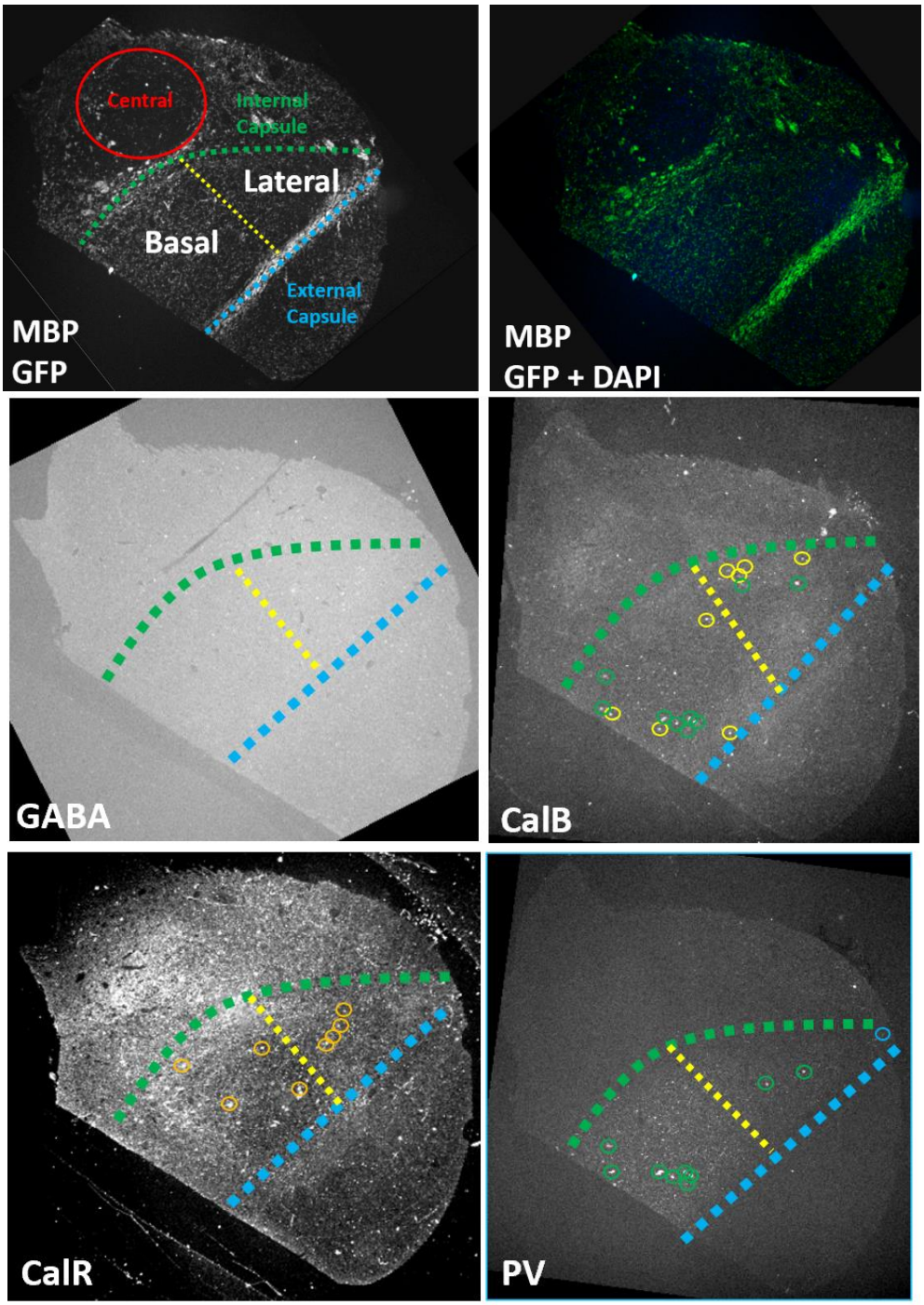

Figure 5. 10X images of MBP (section 1), GABA (section 10), CalB (section 6), PV (section 4), and CalR (section 7) staining in BLA. MBP was used to identify the boundaries of the amygdala. The internal (green) and external (blue) capsules mark the medial and lateral boundaries, respectively, of the basolateral amygdala. The yellow line roughly divides the BLA into lateral and basal nuclei. Central amygdala is outlined in red. GABA images were taken in Texas Red fluorescent channel, MBP/CalB/PV/CalR in GFP. Yellow circles indicate cells that are only CalB+, blue circles are only PV+, green circles indicate CalB and PV colocalization, orange circles indicate CalR+ only cells.

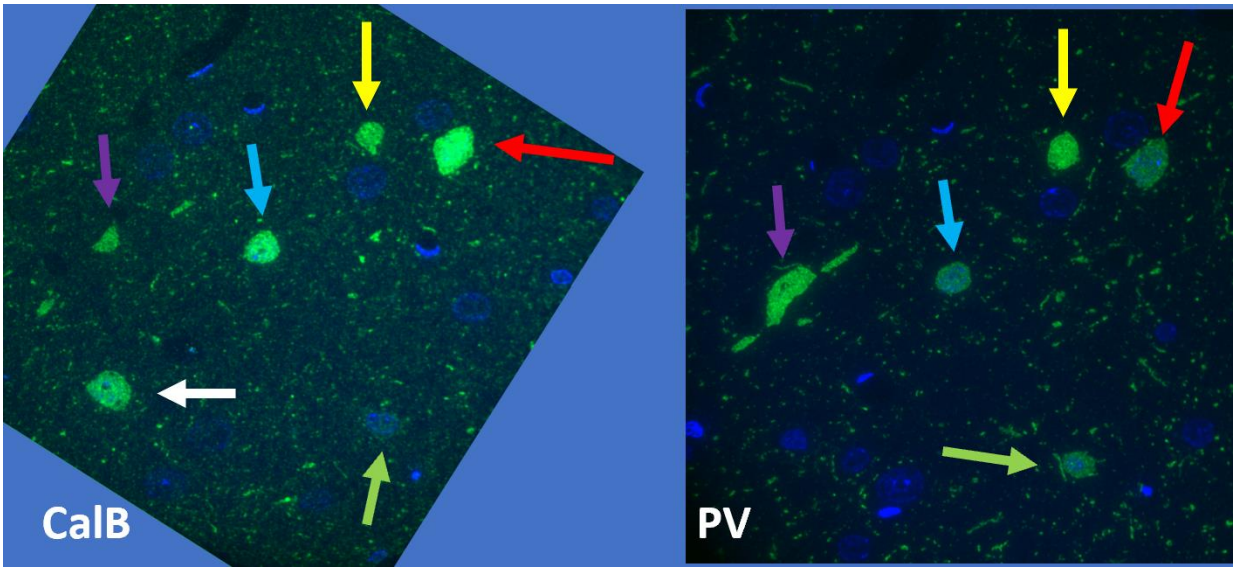

Figure 6. 100x images of CalB and PV staining showing colocalization of CalB and PV. Each unique color of arrow indicates the same cell between sections. The cells indicated by red, yellow, light blue, purple, and light green arrows all express both CalB and PV. However, the cell labeled by the white arrow only expresses CalB (Imaging credit to Rebecca Tripp).

Discussion

The patterns and cell populations displayed in these results follow some of the key trends identified by McDonald: high level of colocalization between CalB and PV, a small subset of PV+/CalB- cells, and no colocalization of CalR+ and CalB+ or PV+ cells. Some differences were observed in the percentages of each category. McDonald observed that of all BLA GABAergic cells, 41.2% were CalB+, 20.5% CalR+, and 19% PV+. While the numbers in this study were significantly lower, the trends were similar. **Figure 7** is a Venn diagram of the relative number of cells expressing calcium-binding proteins based on McDonald's style that reflects the data in this study. When compared to **Figure 2**, it is clear the CalB, CalR, and PV portions of the Venn diagram are very similar. The most prevalent group in each nucleus were CalB+ cells (28.95% in BA, 17.65% in LA), with CalR (10.5% in BA, 11.8% in LA) and PV

(18.4% in BA, 8.8% in LA) close in expression. One explanation for this discrepancy is that McDonald's data comes from averages of a career's worth of data collection throughout the amygdala, while this is obtained from a single experiment at one specific point along the rostro-caudal axis. Given that the expected trends in expression are present, it is likely that analyzing an equivalent amount of data would yield similar results.

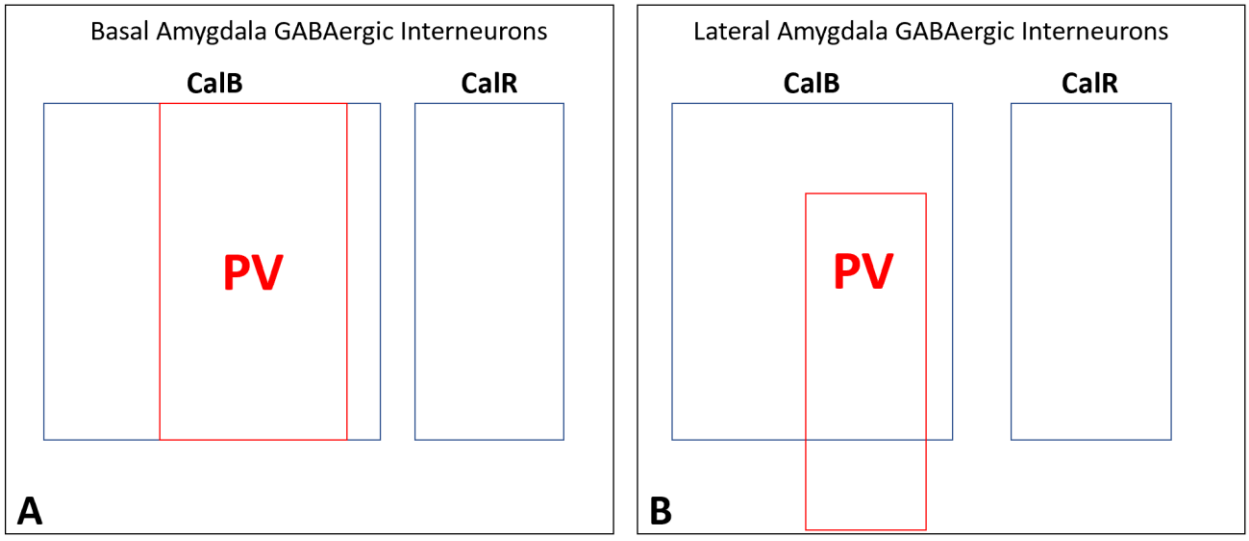

Figure 7. Populations of calcium-binding proteins in basal and lateral amygdala determined by serial multiplex IHC. Each are depicted in their relative ratios. A, In BA, there were 3 clear populations identified: CalB+/PV-, CalB/PV+, and CalR+. B, In LA, these 3 populations were also present, but there was an additional group of PV+/CalB-.

While the data are important, the real success of this study is its potential to transform the field of immunohistochemistry and drastically increase the level of work output and efficiency. In a single rat, thousands of ultrathin sections can be stained for a nearly unlimited number of antibodies. Previous studies would dual-label two antibodies on 50 microns of tissue at a time in order to combine data and form a complete picture of the different interneuron populations. This shows that individual neurons can be followed across 100 nanometer sections to identify the contents of each specific neuron. This has clear advantages in yielding much more data from a given amount of tissue, as well as utilization of many different conditions.

These advantages do not come without challenges, which took significant time to work around. Since serial multiplexing is a novel method, protocols underwent lengthy trial-and-error and fine-tuning. For example, the proper dilutions of each antibody had to be perfected. There are dozens of examples of IHC on thick sections, but ultrathin tissue has less available antigens and requires greater concentrations of antibody to bind. This also led to experimenting with resin removal and antigen retrieval to increase binding sites. While acetone and pressure cooking in acid was determined to yield the best labeling, it was not the case for every antibody. For example, it became clear that GABA antibodies actually labeled better without acetone or pressure cooking, and instead prefer glutaraldehyde and glycine treatment. Incubation times of primary and secondary antibodies were significantly reduced from IHC on thick sections as to reduce extraneous labeling. While this took time to perfect, it resulted in a much more efficient protocol that allows IHC to be completed in a few hours as opposed to multiple days.

Another challenge of ultrathin IHC is collection of the ultrathin sections themselves. Mastering the ultramicrotome is a process that takes several months and requires significant patience. It involves working with a block of tissue only a few millimeters wide, ultrathin sections that are nearly invisible to the naked eye, and extra care not to damage the diamond knife. Additionally, mounting sections on traditional glass slides was determined to be less than ideal for imaging ultrathin sections. Since the tissue is so thin, the sections must be mounted directly on coverslips, so the imaging does not take place through the mounting medium in addition to the glass coverslip.

Finally, it is critical to have confirmation of the labeling that is observed. Cell counting was always done with images of 20x magnification or greater since it is too difficult to differentiate signal from background at 10x. Even at 20x, higher magnification images of 40x or

100x were almost always used to confirm the labeling. **Figure 8** shows how the image significantly increases in clarity from 10x to 20x to 40x to 100x. However, even at 100x, additional levels of verification are required. The 100x GFP image appears to show 5 clearly labeled cell bodies. When overlayed with the same field in the DAPI channel, it becomes ambiguous with two apparently labeled cells missing nuclei. They label an area of the tissue where the nucleus is absent either because this slice of tissue does not contain it, or there is no cell in that location at all. As a result, a nearby serial section with the same primary antibody must be used for comparison. In the example in **Figure 8**, the following serial section had been labeled for the same antibody and allowed for verification of the cell labeling. Because of this common occurrence in IHC of imperfect labeling, it requires experience and multiple levels of verification before drawing definite conclusions.

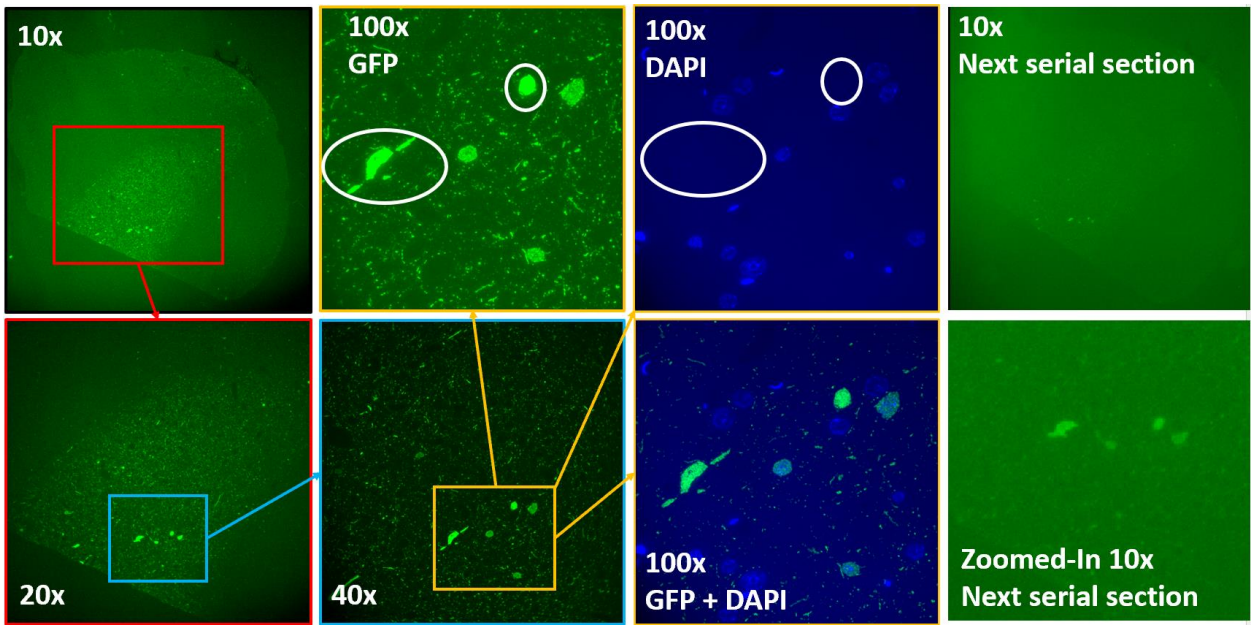

Figure 8. 10x, 20x, 40x, & 100x images of PV staining. This figure demonstrates the need for multiple levels of verification in determining correct immunolabeling. In the 100x GFP image, there appear to be 5 PV+ cells, however the DAPI channel shows there are no actual nuclei located at those apparent cells circled in white. As a result, the next immediate serial section (also labeled for PV) is used to determine if the labeling pattern is consistent. In this case, the same cells are immunolabeled, indicating a faithful labeling pattern (Imaging credit to Rebecca Tripp for 40x & 100x images).

Future Directions

While there are certainly challenges involved in serial multiplex IHC, there are clear benefits to the method that open the door to new possibilities. By employing these methods, the limited study done in this thesis can be expanded for a multitude of cell-type markers. This includes the neuropeptides that have shown to colocalize with calcium-binding proteins. For example, SOM, NPY, and CCK with CalB, and VIP and CCK with CalR. What others have achieved across several years of work can be replicated and expanded in less than a week through serial multiplex IHC.

Another important application of this method would be to compare sex differences in the BLA. Very few studies have attempted to characterize the interneuronal subpopulations in females as compared to males. This could also incorporate additional factors, such as estrous cycle stage or behavioral conditions.

There are nearly unlimited neuropeptides and receptors that would be interesting and useful to analyze on a large scale, but the following are of particular relevance to amygdala circuitry, learning, and psychiatric/neurological disorders: calcium/calmodulin-dependent protein kinase II (CaMKII), a protein involved in many functions such as plasticity, synaptic activity, gene expression, and signaling cascades (Shioda and Fukunaga, 2018); Forkhead box protein P2 (FOXP2), an important transcription factor involved in brain activity (Den Hoed et al., 2021); c-fos, the protein product of a proto-oncogene that marks neuronal activity (Bullitt, 1990); vesicular glutamate transporters (VGLUT1 and VGLUT2) to identify excitatory synapses and their relation to the interneuron populations (Herzog et al., 2006); vesicular GABA transporter (VGAT) to identify GABAergic synapses in addition to the previously identified GABA+ cell bodies (Wang et al., 2009); serotonin transporter (SERT), a marker of the neurotransmitter

serotonin, which has been linked to a variety of neurological and psychiatric diseases (Kish et al., 2005); norepinephrine transporter (NET), a marker of the neurotransmitter norepinephrine, which mediates behaviors such as mood and depression (Bönisch and Brüss, 2006); neurokinin-1 receptor (NK-1R), which plays a role in stress response and pain (Duric and McCarson, 2005); cannabinoid 1 receptor (CB1R), a potential factor in schizophrenia (Eggan et al., 2008); calcitonin gene-related peptide (CGRP), which plays a role in migraines (Warfvinge and Edvinsson, 2017); estrogen receptors alpha and beta (ERα and ERβ), indicators of the effect of estrogen on the brain (Pérez et al., 2003); androgen receptor, which is suggested to play a significant role in synaptic plasticity (Hajszan et al., 2008); and dopamine receptors 1 and 2 (D1R and D2R) and dopamine transporter (DAT), which are highly linked to addictive behaviors and the reward pathway in the brain (Drago et al., 1998). Many if not all of these have been proposed or proven to play important roles in a variety of psychiatric and neurological diseases. Since the amygdala is implicated in many of these diseases as well, it would be a fascinating study to identify the relationship between all of these and how they are expressed in the different interneuron populations. The high-volume capacity of serial multiplex IHC allows for in-depth studies of significant neurobiological and psychiatric relevance to be possible.

References

Bauer, E.P., Schafe, G.E., and LeDoux, J.E. (2002) NMDA receptors and L-type voltage-gated calcium channels contribute to long-term potentiation and different components of fear memory formation in the lateral amygdala. *The Journal of Neuroscience* 22(12):5239-5249.

Bissiere, S., Humeau, Y., and Lüthi, A. (2003) Dopamine gates LTP induction in lateral amygdala by suppressing feedforward inhibition. *Nature Neuroscience* 6(6):587-592.

Blume, S.R., Freedberg, M., Vantrease, J.E., Chan, R., Padival, M., Record, M.J., DeJoseph, M.R., Urban, J.H., & Rosenkranz, J.A. (2017) Sex- and estrus-dependent differences in rat basolateral amygdala. *Journal of Neuroscience*, 37(44):10567-10586.

Bönisch, H. and Brüss, M. (2006) The norepinephrine transporter in physiology and disease. *Neurotransmitter Transporters* 175:485-524.

Brinley-Reed, M., Mascagni, F., and McDonald, A.J. (1995) Synaptology of prefrontal cortical projections to the basolateral amygdala: an electron microscopic study in the rat. *Neuroscience Letters* 202:45-48.

Bullitt, E. (1990) Expression of c-fos-like protein as a marker for neuronal activity following noxious stimulation in the rat. *Journal of Comparative Neurology* 296(4):517-530.

Carlsen, J. (1988) Immunocytochemical localization of glutamate decarboxylase in the rat

basolateral amygdaloid nucleus, with special reference to GABAergic innervation of amygdalostriatal projection neurons. *Journal of Comparative Neurology* 273:513-526.

Carlsen, J. and Heimer, L. (1988) The basolateral amygdaloid complex as a cortical-like structure. *Brain Research* 441:377-380.

Den Hoed, J., Devaraju, K., & Fisher, S.E. (2021) Molecular networks of the FOXP2 transcription factor in the brain. *EMBO Reports* 22:1-15.

Deshmukh, A., Rosenbloom, M.J., Sassoon, S., O'Reilly, A., Pfefferbaum, A., & Sullivan, E.V. (2003) Alcoholic men endorse more DSM-IV withdrawal symptoms than alcoholic women matched in drinking history. *Journal of Studies on Alcohol*, 64(3):375-379.

Drago, J., Padungchaichot, P., Accili, D., & Fuchs, S. (1998) Dopamine receptors and dopamine transporter in brain function and addictive behaviors: Insights from targeted mouse mutants. *Developmental Neuroscience* 20:188-203.

Duric, V. and McCarson, K.E. (2005) Hippocampal neurokinin-1 receptor and brain-derived neurotrophic factor gene expression is decreased in rat models of pain and stress. *Neuroscience* 133:999-1006.

Eggan, S.M., Hashimoto, T., & Lewis, D.A. (2008) Reduced cortical cannabinoid 1 receptor messenger RNA and protein expression in schizophrenia. *Archives of General Psychiatry* 65(7):772-784.

Erol, A., & Karpyak, V.M. (2015) Sex and gender-related differences in alcohol use and its consequences: Contemporary knowledge and future research considerations. *Drug and Alcohol Dependence*, 156:1-13.

Farb, C.R. and LeDoux, J.E. (1999) Afferents from rat temporal cortex synapse on lateral amygdala neurons that express NMDA and AMPA receptors. *Synapse* 33:218-229.

Fuller, T.A., Russchen, F.T., Price, J.L. (1987) Sources of presumptive glutamatergic/aspartergic afferents to the rat ventral striatopallidal region. *Journal of Comparative Neurology* 258:317-338.

Hajszan, T., MacLusky, N.J., & Leranth, C. (2008) Role of androgens and the androgen receptor in remodeling of spine synapses in limbic brain areas. *Hormones and Behavior* 53:638-646.

Hall, E. (1972) The amygdala of the cat: a Golgi study. *Cell and Tissue Research* 134:439-458.

Herry, C., Ferraguti, F., Singewald, N., Letzkus, J.J., Ehrlich, I., & Lüthi, A. (2010) Neuronal circuits of fear extinction. *The European Journal of Neuroscience*, 31: 599-612.

Herzog, E., Takamori, S., Jahn, R., Brose, N., & Wojcik, S.M. (2006) Synaptic and vesicular co-localization of the glutamate transporters VGLUT1 and VGLUT2 in the mouse hippocampus. *Journal of Neurochemistry* 99(3): 1011-1018.

Kemppainen, S. and Pitkänen, A. (2000) Distribution of parvalbumin, calretinin, and calbindin-

D28k immunoreactivity in the rat amygdaloid complex and colocalization with gamma-aminobutyric acid. *Journal of Comparative Neurology* 426:441-467.

Kessler, R.C., Berglund, P., Demler, O., Jin, R., Merikangas, K.R., & Walters, E.E. (2005) Lifetime prevalence and age-of-onset distributions of DSM-IV disorders in the national comorbidity Survey replication. *Archives of General Psychiatry*, 62(6):593-602.

Kessler, R.C., Petukhova, M., Sampson, N.A., Zaslavsky, A.M., & Wittchen, H.-U. (2012) Twelve-month and lifetime prevalence and lifetime morbid risk of anxiety and mood disorders in the United States. *International Journal of Methods in Psychiatry Research*, 21(3):169-184.

Kish, S.J., Furukawa, Y., Chang, L.-J., Tong, J., Ginovart, N., Wilson, A., Houle, S., & Meyer, J.H. (2005) Regional distribution of serotonin transporter protein in postmortem human brain: Is the cerebellum a SERT-free brain region?. *Nuclear Medicine and Biology* 32:123-128.

Lang, E.J. and Paré, D. (1998) Synaptic responsiveness of interneurons of the cat lateral amygdaloid nucleus. *Neuroscience* 83(3):877-889.

LeDoux, J. (2000). The amygdala and emotion: A view through fear. In Aggleton JP (Ed.), *The amygdala* (2nd ed., pp. 289-310). Oxford: Oxford University Press.

LeDoux, J.E., Farb, C.F., and Milner, T.A. (1991) Ultrastructure and synaptic associations of auditory thalamo-amygdala projections in the rat. *Experimental Brain Research* 85:577-

586.

Mascagni, F. and McDonald, A.J. (2003) Immunohistochemical characterization of cholecystokinin containing neurons in the rat basolateral amygdala. *Brain Research* 976:171-184.

McDonald, A.J. (1982) Neurons of the lateral and basolateral amygdaloid nuclei: a Golgi study in the rat. *Journal of Comparative Neurology* 212:293-312.

McDonald, A.J. (1984) Neuronal organization of the lateral and basolateral amygdaloid nuclei in the rat. *Journal of Comparative Neurology* 222:589-606.

McDonald, A.J. (1992) Projection neurons of the basolateral amygdala: a correlative Golgi and retrograde tract tracing study. *Brain Research Bulletin* 28(2):179-185.

McDonald, A.J. (1996) Glutamate and aspartate immunoreactive neurons of the rat basolateral amygdala: colocalization of excitatory amino acids and projections to the limbic circuit. *The Journal of Comparative Neurology* 365:367-379.

McDonald, A.J. (2020) Functional neuroanatomy of the basolateral amygdala: neurons, neurotransmitters, and circuits. *Handbook of Behavioral Neuroscience*, 26: 1-38.

McDonald, A.J. (2021) Immunohistochemical identification of interneuronal subpopulations in the basolateral amygdala of the rhesus monkey (*Macaca mulatta*). *Neuroscience*, 455:113-127.

McDonald, A.J. and Augustine, J.R. (1993) Localization of GABA-like immunoreactivity in the monkey amygdala. *Neuroscience* 52(2):281-294.

McDonald, A.J. and Mascagni, F. (2001a) Colocalization of calcium-binding proteins and GABA in neurons of the rat basolateral amygdala. *Neuroscience* 105(3):681-693.

McDonald, A.J. and Mascagni, F. (2001b) Localization of the CB1 type cannabinoid receptor in the rat basolateral amygdala: high concentrations in a subpopulation of cholecystokinin-containing interneurons. *Neuroscience* 107(4):641-652.

McDonald, A.J. and Mascagni, F. (2002) Immunohistochemical characterization of somatostatin containing interneurons in the rat basolateral amygdala. *Brain Research* 943(2):237-244.

McDonald, A.J. and Pearson, J.C. (1989) Coexistence of GABA and peptide immunoreactivity in non-pyramidal neurons of the basolateral amygdala. *Neuroscience Letters* 100:53-58.

McDonald, A.J., Muller, J.F., and Mascagni, F. (2002) GABAergic innervation of alpha type II calcium/calmodulin-dependent protein kinase immunoreactive pyramidal neurons in the rat basolateral amygdala. *Journal of Comparative Neurology* 446:199-218.

Mears, D. & Pollard, H.B. (2016) Network science and the human brain: Using graph theory to understand the brain and one of its hubs, the amygdala, in health and disease. *Journal of Neuroscience Research*, 94: 590-605.

Millhouse, O.E. and DeOlmos, J. (1983) Neuronal configurations in lateral and basolateral

amygdala. *Neuroscience* 10(4):1269-1300.

Muller, J.F., Mascagni, F., and McDonald, A.J. (2006) Pyramidal cells of the rat basolateral amygdala: synaptology and innervation by parvalbumin-immunoreactive interneurons. *Journal of Comparative Neurology* 494:635-650.

Pape, H.C. & Paré, D. (2010) Plastic synaptic networks of the amygdala for the acquisition, expression, and extinction of conditioned fear. *Physiological Reviews*, 90: 419-463.

Paré, D. and Smith, Y. (1993) Distribution of GABA immunoreactivity in the amygdaloid complex of the cat. *Neuroscience* 57(4):1061-1076.

Paré, D., Smith, Y., and Paré, J.F. (1995) Intra-amygdaloid projections of the basolateral and basomedial nuclei in the cat: Phaseolus vulgaris-leucoagglutinin anterograde tracing at the light and electron microscopic level. *Neuroscience* 69:567-583.

Paxinos, G. & Watson, C. (1997) *The rat brain in stereotaxic coordinates*. New York: Academic Press.

Pérez, S.E., Chen, E.-Y., & Mufson, E.J. (2003) Distribution of estrogen receptor alpha and beta immunoreactive profiles in the postnatal rat brain. *Developmental Brain Research* 145:117-139.

Pitkänen, A. (2000) Connectivity of the rat amygdala. In Aggleton JP (Ed.), *The amygdala* (2nd ed., pp. 31-116). Oxford: Oxford University Press.

Roberts, G.W., Woodhams, P.L, Polak, J.M., and Crow, T.J. (1982) Distribution of neuropeptides in the limbic system of the rat: the amygdaloid complex. *Neuroscience* 7:99-131.

Rodrigues, S.M., Bauer, E.P., Farb, C.R., Schafe, G.E., and LeDoux, J.E. (2002) The group I metabotropic glutamate receptor mGluR5 is required for fear memory formation and long-term potentiation in the lateral amygdala. *The Journal of Neuroscience* 22(12):5219-5229.

Równiak, M., Bogus-Nowakowska, K., & Robak, A. (2015) The densities of calbindin and parvalbumin, but not calretinin neurons, are sexually dimorphic in the amygdala of the Guinea pig. *Brain Research*, 1604:84-97.

Shioda, N. and Fukunaga, K. (2018) Physiological and Pathological Roles of CaMKII-PP1 Signaling in the Brain. *International Journal of Molecular Sciences* 19(1), 20:1-10.

Smith, Y. and Paré, D. (1994) Intra-amygdaloid projections of the lateral nucleus in the cat: PHA-L anterograde labeling combined with postembedding GABA and glutamate immunocytochemistry. *Journal of Comparative Neurology* 342:232-248.

Smith, Y., Paré, J.F., and Paré, D. (2000) Differential innervation of parvalbumin-immunoreactive interneurons of the basolateral amygdaloid complex by cortical and intrinsic inputs. *Journal of Comparative Neurology* 416:496-508.

Stefanacci, L., Farb, C.R., Pitkanen, A., Go, G., LeDoux, J.E., and Amaral, D.G. (1992) Projections from the lateral nucleus to the basal nucleus of the amygdala: a light and electron microscopic PHA-L study in the rat. *Journal of Comparative Neurology* 323:586-601.

Stutzmann, G.E. and LeDoux, J.E. (1999) GABAergic antagonists block the inhibitory effects of serotonin in the lateral amygdala: a mechanism for modulation of sensory inputs related to fear conditioning. *The Journal of Neuroscience* 19:RC8(1-4).

Substance Abuse and Mental Health Services Administration. (2019) Results from the 2018 national Survey on drug use and health. Detailed tables. https://www.samhsa.gov/data/report/2018-nsduh-detailed-tables.

Tovote, P., Fadok, J.P., & Lüthi, A. (2015) Neuronal circuits for fear and anxiety. *Nature Reviews Neuroscience*, 16: 317-331.

Wang, Y., Kakizaki, T., Sakagami, H., Saito, K., Ebihara, S., Kato, M., Hirabayashi, M., Saito, Y., Furuya, N., & Yanagawa, Y. (2009) Fluorescent labeling of both GABAergic and glycinergic neurons in vesicular GABA transporter (VGAT)-Venus transgenic mouse. *Neuroscience* 164(3):1031-1043.

Warfvinge, K. & Edvinsson, L. (2017) Distribution of CGRP and CGRP receptor components in the rat brain. *Cephalagia* 39(3):342-353.

Ziel, R. (2013) Principle of sample movement in making a cut on a rotary microtome. Wikimedia Commons. Retrieved April 5, 2022. https://commons.wikimedia.org/wiki/File:Microtome_principle.svg